LIMNOLOGY and OCEANOGRAPHY

ASLO

Limnol. Oceanogr. 69, 2024, 2680–2687

doi: 10.1002/lno.12696

Connectivity between Siberian river runoff and the lower limb of the Atlantic Meridional Overturning Circulation

Caroline V. B. Gjelstrup,[1*] **Paul G. Myers**,[2] **Craig M. Lee**,[3] **Kumiko Azetsu-Scott**,[4] **Colin A. Stedmon**[1]
[1]National Institute of Aquatic Resources, Technical University of Denmark, Denmark
[2]Department of Earth and Atmospheric Sciences, University of Alberta, Edmonton, Canada
[3]Applied Physics Laboratory, University of Washington, Seattle, Washington, USA
[4]Fisheries and Ocean Canada, Bedford Institute of Oceanography, Dartmouth, Nova Scotia, Canada

Abstract

Freshwater from the Arctic participates in the globally important Atlantic Meridional Overturning Circulation (AMOC). We use high-resolution, in situ observations of dissolved organic matter (DOM) fluorescence to trace the origins of freshwater and organic carbon in the densest component of the AMOC, namely Denmark Strait Overflow Water (DSOW). We find a distinct terrestrial DOM signal in DSOW and trace it upstream to the Siberian shelves in the Arctic Ocean. This implies a riverine origin of freshwater in DSOW. We estimate that the Siberian Shelf water contribution constitutes approximately 1% of DSOW. Ocean circulation modeling confirms the inferred pathway and highlights Denmark Strait as an important location for the entrainment of the riverine signal into DSOW. Our proposed method can be deployed on a range of observing systems to elucidate freshwater dispersion across the Arctic and subarctic, thereby contributing to the broader discussion on freshwater impacts and organic carbon sequestration in the AMOC.

The Atlantic Meridional Overturning Circulation (AMOC) is a large-scale system of currents responsible for redistributing heat, salt, oxygen, and carbon on global and centennial scales. The upper limb of the AMOC brings warm, saline subtropical waters to the high-latitude North Atlantic and Arctic, where they are transformed by strong heat loss and various processes affecting salinity, such as precipitation, runoff from land, and sea-ice formation and melt. The cold, dense waters that result from these transformations return equatorward at depth (Buckley and Marshall 2016). This process regulates Earth's climate by bringing heat to the North Atlantic and exporting oxygen and carbon to the deep. Freshwater from the central Arctic Ocean participates in this overturning circulation. Tracer studies have shown that a contribution of relatively fresh waters from the Arctic is necessary to replicate the properties of Denmark Strait Overflow Water (DSOW), which is at once the densest and volumetrically greatest contributor to the lower limb of the AMOC (Dickson and Brown 1994; Edmonds et al. 2001; Tanhua et al. 2005). In addition, analysis of lignin content in deep waters suggested a riverine contribution to the overflow waters (Benner et al. 2005). Similarly, a recent study showed that about half of the freshwater exiting the central Arctic Ocean via Fram Strait must be stirred into the deep in order to close the Nordic Seas freshwater budget (Le Bras et al. 2021). However, to further resolve the influence of Arctic freshwater on the overturning circulation, it is necessary to source fractionate the freshwater contributions.

In this study, we seek to uncover the origins of the Arctic freshwater involved in the overturning circulation. Gaining insights into these origins will benefit our ability to predict changes in the export of freshwater, oxygen, and carbon as the Arctic hydrological cycle changes. To this end, we take advantage of the fluorescent properties of dissolved organic matter (DOM), which have proven a promising tracer of Arctic waters over the past two decades (Amon et al. 2003; Granskog et al. 2012; Stedmon et al. 2021). There are two overarching sources of DOM fluorescence to consider. The first is autochthonous, representing material that is produced within a given water body. This contribution is both directly produced by organisms at all levels of the marine food web, and also a

*Correspondence: cvbgj@aqua.dtu.dk

Additional Supporting Information may be found in the online version of this article.

Author Contribution Statement: CVBG: Conceptualization; Methodology; Formal analysis; Investigation; Visualization; Writing – original draft; Writing – review and editing. PGM: Formal analysis; Investigation; Visualization; Writing – review and editing. CML: Investigation; Funding acquisition; Writing – review and editing. KAS: Investigation; Funding acquisition; Writing – review and editing. CAS: Conceptualization; Methodology; Funding acquisition; Writing – review and editing.

product of the microbial turnover of organic matter in pelagic and benthic environments (Stedmon and Nelson 2015). In deep waters beyond the reaches of light, this is primarily produced by microbes degrading sinking particulate organic matter or labile DOM. The second source is allochthonous (or preformed) and represents material generated outside the bounds of the system under study. This is typically dominated by DOM fluorescence associated with river discharge and has, for the most part, been leached from soils (Stedmon and Nelson 2015).

The Arctic Ocean is unique in that it receives a comparatively large contribution of terrestrial DOM. Due to its stratification, the signal is retained in surface water layers (~500 m) and widespread across much of the basin (Amon and Benner 2003; Benner et al. 2005). DOM delivered by rivers to the shallow Siberian shelves is rejected in brine during sea-ice formation, resulting in DOM-rich Siberian Shelf water, which is subsequently exported off the shelf (Stedmon et al. 2021). These waters are transported across the central Arctic Ocean with the Transpolar Drift and exit via Fram Strait as Polar Surface Water in the East Greenland Current (Fig. 1a; Granskog et al. 2012). In contrast to autochthonous DOM, terrestrial DOM is present in the water at the time of water mass formation and sinking. Lending terminology from the use of conservative inorganic nutrient tracers (Broecker 1974), this DOM pool can be thought of as initial or preformed DOM. Other sources of freshwater in the Arctic, including sea-ice melt and precipitation, are, in comparison, insignificant sources of DOM (Anderson and Amon 2015; Stedmon et al. 2021).

Here, we present in situ DOM fluorescence measurements taken in the subarctic northern Labrador Sea. The high vertical resolution offered by the in situ fluorometer provides confidence that the observations resolve DOM variability. We find that despite extensive dilution and mixing with ambient water masses, the DOM signature unique to low-salinity Arctic waters persists across the Arctic–subarctic boundary and can be traced with the outflow on either side of Greenland into the Labrador Sea. We then present evidence of terrestrial DOM in dense DSOW and trace this signal upstream to its riverine source on the Siberian shelves in the central Arctic Ocean. Model simulations using a passive tracer tagging buoyant river runoff corroborate the pathway inferred from observational data. The work presented here demonstrates biogeochemical connectivity at large regional scales and provides insights into the transport and partitioning of Arctic freshwater and organic carbon in the global overturning circulation.

Methods

Hydrographic data

The hydrographic data analyzed in this study were collected aboard RV *Neil Armstrong* in October 2022 as part of the Davis Strait Program. The survey included 26 stations

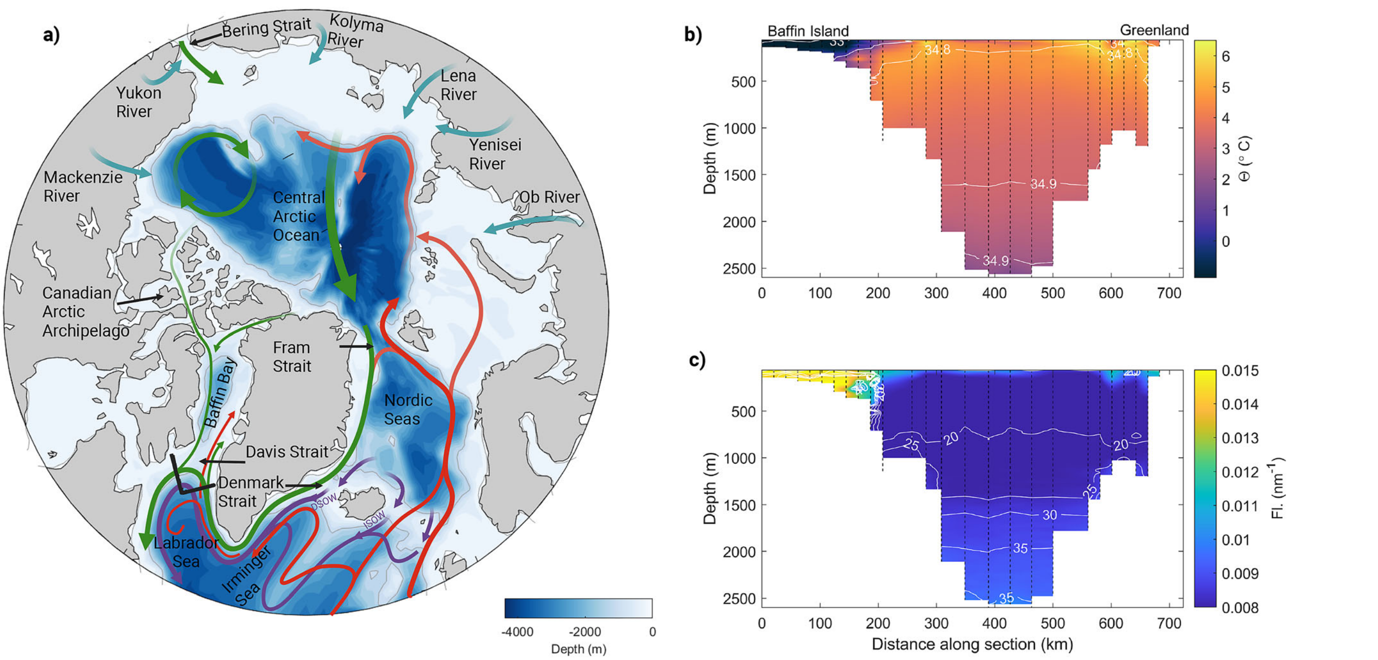

Fig. 1. Schematic of circulation in the Arctic and Subpolar North Atlantic (**a**). Blue arrows are major Arctic rivers, green arrows represent circulation of low salinity water, red arrows denote Atlantic-origin water and purple arrows show dense overflow water pathways. Denmark Strait Overflow Water (DSOW) and Iceland Scotland Overflow Water (ISOW) are indicated. The hydrographic transect discussed in this paper is shown in black. Panel (**b**) displays the temperature distribution along the transect annotated with practical salinity contours. Panel (**c**) displays DOM fluorescence (Fl.) intensity with contours of apparent oxygen utilization (AOU, μmol kg^{-1}) overlain. Black stippled lines on (**b**) and (**c**) indicate sampling locations.

distributed along a transect crossing the northern Labrador Sea (Fig. 1a). Data were acquired using a Sea-Bird 911+ conductivity–temperature–depth (CTD) with estimated accuracies of $\pm 0.001°C$, ± 0.003, and ± 1.5 dbar for temperature, practical salinity (S_p) and pressure, respectively. Dissolved oxygen measurements were obtained with a Sea-Bird SBE 43 dissolved oxygen sensor with an accuracy of $\pm 2\%$ saturation and calibrated using the Winkler titration method. In addition, high-resolution in situ DOM fluorescence measurements were obtained with a Wetlabs ECO FL(RT)D fluorometer operating on the excitation 370-nm and emission 460-nm wavelength pair and with a sensitivity of 0.09 ppb. These data were calibrated to laboratory measurements of DOM fluorescence made using a Horiba Aqualog fluorometer and pure water as a blank and reference (Lawaetz and Stedmon 2009). The effect of particles on the in situ fluorometer output can be neglected since the sampling stations are far from the coast, and our focus is on the deep waters. In addition, the influence of temperature was found to be insignificant and was therefore excluded from the calibration. The DOM fluorescence profiles were smoothed with a moving average algorithm with a vertical window length of 10 m to suppress noise.

Numerical model

We compare the in situ observations with a numerical simulation of Eurasian river runoff. We use the ANHA12-ECP024 simulation, which covers the Arctic and Atlantic Oceans with a 1/12° horizontal resolution and 50 depth levels. The simulation uses the NEMO 3.6 ocean modeling framework (Madec 2008) and sea-ice model (LIM2; Fichefet and Maqueda 1997). It has two open boundaries: one at 20°S and the other at Bering Strait. Boundary and initial conditions were set based on the ECMWF ORAS5 ensemble member product (https://doi.org/10.21957/la2v0442). The Eurasian river runoff tracer was released as a passive tracer in the near-surface layer at the location of Siberian rivers. The amount of tracer released in each grid cell and time step is proportional to the river runoff (Hu et al. 2019) and its evolution is described by advection and diffusion equations for temperature and salinity. Further details on the numerical model are provided in the Supporting Information.

Results and discussion

Water masses and circulation

The Labrador Sea is a useful point of observation, serving as a node between time-varying inputs of water masses from the Arctic and sub-Arctic seas and a starting point of the global overturning circulation. The relatively fresh outflow from the central Arctic Ocean is focused toward the Labrador Sea due to the clockwise circulation around Greenland with the East Greenland Current and subsequent transport with the West Greenland Current (Fig. 1a). A part of this flow recirculates across the northern Labrador Sea whilst the rest continues north along the west coast of Greenland (Fig. 1a). Despite modification and severe dilution with surrounding waters, the DOM signal in these waters is retained as evident from the elevated DOM fluorescence apparent near the surface at the eastern boundary of the transect on the West Greenland shelf (Fig. 1c). The Labrador Sea also receives low-salinity Arctic outflow channeled through the Canadian Arctic Archipelago and along the western Baffin Bay with the Baffin Island Current (Fig. 1a). These waters carry a strong DOM fluorescence signal, which is largely confined to the shallow western shelf of the Davis Strait (Fig. 1c).

Weakly stratified waters formed locally via convective processes occupy the intermediate depth range. These waters are recently ventilated as indicated by their low apparent oxygen utilization (20–30 μmol kg^{-1}), and are characterized by very low DOM fluorescence (Fig. 1c). A salinity maximum below this layer denotes Northeast Atlantic Deep Water (Figs. 1b, 2a). Northeast Atlantic Deep Water is a product of

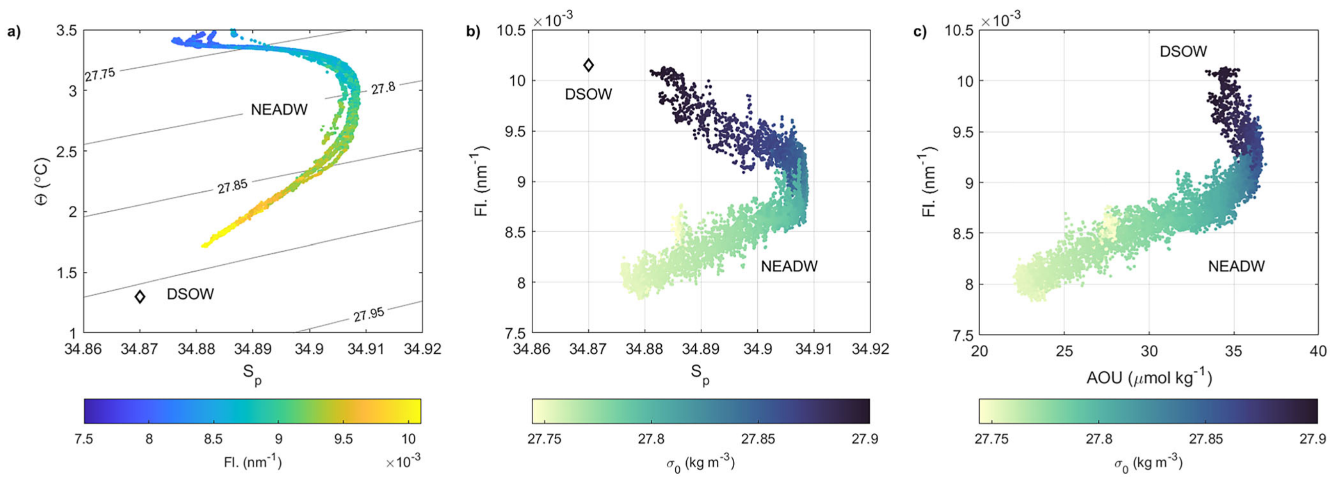

Fig. 2. Hydrographic properties below 1200 m depth shown in: θ–S_p space (**a**), Fl.–S_p space (**b**), and Fl.–AOU space (**c**). Northeast Atlantic Deep Water (NEADW) and projected Denmark Strait Overflow Water (DSOW) are indicated.

Iceland-Scotland Overflow Water and ambient North Atlantic waters entrained as the overflow plume spills across the Greenland-Scotland Ridge east of Iceland and circulates along the perimeter of the Irminger Sea (Fig. 1a; Yashayaev and Dickson 2008). Once reaching the Southeast Greenland slope, it meets and overlies the slightly fresher yet denser DSOW (Dickson and Brown 1994). DSOW is a combination of several water masses originating in the central Arctic Ocean and Nordic Seas, fed toward the Denmark Strait with the North Icelandic Jet and East Greenland Current (Tanhua et al. 2005; Våge et al. 2011). Whilst the core of DSOW was not sampled at the northern Labrador Sea transect (Fig. 1a), a mixture of Northeast Atlantic Deep Water and DSOW is present in the dataset (Fig. 2a). Assuming a core DSOW salinity of 34.87, DSOW is projected in θ–S space. Note that the salinity of DSOW varies on seasonal and interannual timescales (Tanhua et al. 2005; Opher et al. 2022). We use 34.87 reported as the mean salinity when varying East Greenland Current and North Icelandic Jet contributions are accounted for (Opher et al. 2022). Together, Northeast Atlantic Deep Water and DSOW constitute North Atlantic Deep Water and what eventually becomes the headwaters of the AMOC.

Differentiation of preformed and autochthonous DOM in DSOW

DOM fluorescence in the dense waters display apparent conservative behavior relative to salinity (Fig. 2b) but with opposing relationships for waters above and below the Northeast Atlantic Deep Water salinity maximum. Above the less dense water has lower DOM fluorescence resulting in an increase in fluorescence with mixing, while DOM fluorescence is higher in DSOW below.

Both apparent oxygen utilization and DOM fluorescence increase through the Northeast Atlantic Deep Water layer toward the bottom (Fig. 1c). Further analysis of the two mixing lines in Fig. 2b reveals a strong positive correlation with apparent oxygen utilization in Northeast Atlantic Deep Water with $\sigma_0 < 27.85$ kg m^{-3} in particular (Fig. 2c). This is expected and has been documented for the global ocean in general (Yamashita and Tanoue 2008; Jørgensen et al. 2011; Catalá et al. 2015). The trend is attributed turnover of DOM by microbes leading to increased apparent oxygen utilization and accumulation of a DOM fluorescence signal (Jørgensen et al. 2014). However, this trend does not persist for all North Atlantic deep waters (Jørgensen et al. 2011), as clearly shown in Fig. 2c, which exhibits a kink in DOM fluorescence intensity around 9×10^{-3} nm^{-1}. This indicates entrainment of allochthonous (preformed) DOM associated with the mixing of Northeast Atlantic Deep Water with DSOW, drawing DOM fluorescence up beyond what can be explained by microbial processing of organic material. A mixing line is drawn through Northeast Atlantic Deep Water by means of linear regression, and DOM fluorescence in the projected DSOW end-member is estimated by regression at $S = 34.87$. Only data points with little to no influence of autochthonous DOM fluorescence are used. This selection is satisfied by determining the maximum density threshold beyond which the correlation between apparent oxygen utilization and DOM fluorescence breaks down. The threshold density was found to be $\sigma_0 = 27.85$ (kg m^{-3}), thus all lighter waters were excluded. In addition, observations within 20 m from the bottom were excluded as a precautionary measure to avoid potential contamination or distortion from DOM in suspended sediments. Figure 3 shows the resultant mixing line extrapolated to lower salinities and compared with observations from the central Arctic Ocean.

Connectivity with Siberian Shelf water

DOM fluorescence in the dense Labrador Sea observations is generally low compared to that in observations from the central Arctic Ocean. However, at equivalent salinities, DOM fluorescence intensities are comparable and exhibit similar relations to salinity (Fig. 3). This becomes particularly apparent when extrapolating the mixing line to lower salinity values. The mixing line tracks the upper branch of data points in the central Arctic Ocean dataset corresponding to the distribution of DOM fluorescence and salinity observed in the Transpolar Drift (Fig. 3). Furthermore, average DOM fluorescence in Siberian Shelf water close to the Lena River delta was reported at 0.125 nm^{-1} for salinities of 30, and 1.9 nm^{-1} for the Lena River (Walker et al. 2013; Gonçalves-Araujo et al. 2015). Whilst our mixing line aligns well with the Siberian Shelf water endmember, it underestimates the Lena River endmember. This is likely because the observed DOM fluorescence signal has contributions from other rivers with different endmember values and is influenced by sea-ice melt, drawing DOM fluorescence down relative to the Lena River. That Siberian Shelf waterfalls on the mixing line derived from dense Labrador Sea observations implies connectivity between the two, and suggests that preformed DOM present in DSOW is of terrestrial origins supplied via Siberian rivers.

The Siberian Shelf water contribution to DSOW can be determined from the mixing line by estimating endmember properties. Using the saline DOM-poor Northeast Atlantic Deep Water ($S = 34.9$ and Fl. $= 0.009$ nm^{-1}) and the comparatively fresh DOM-rich Siberian Shelf water ($S = 30$, Fl. $= 0.125$ nm^{-1}, and DOC $= 170$ μmol L^{-1}) as endmembers, the Siberian Shelf water contribution to DSOW is estimated at 0.9%. Whilst this estimate is clearly dependent on endmember definitions, we note it is in close agreement with a previous study reporting 1% Polar Surface Water in DSOW based on anthropogenic 129-iodine (Edmonds et al. 2001), thus further lending confidence to our approach. Using the same Siberian Shelf water endmember to derive a ratio of terrestrial DOC to DOM fluorescence, we estimate the terrestrial DOC contents of DSOW at 1.8 μmol L^{-1}. This corresponds to an annual export of 1.9 Tg carbon when assuming a conservative DSOW volume flux of 2.9 Sv (Våge et al. 2011). This is in good agreement with a previous lignin-based estimate of

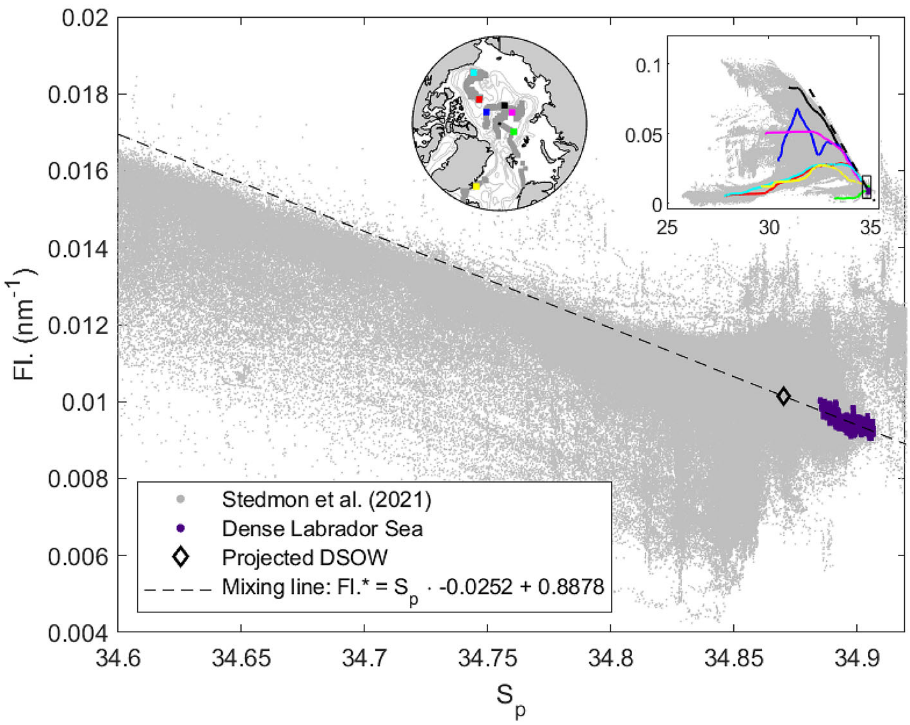

Fig. 3. Comparison of central Arctic Ocean (gray) and dense ($\sigma_0 > 27.85$) waters in the northern Labrador Sea (purple) in Fl.–S_p space. The black diamond indicates Denmark Strait Overflow Water (DSOW) projected into DOM Fl.–S_p space (as in Fig. 2b), and the stippled line shows the mixing line fitted through the dense Labrador Sea observations. The inserts show the spatial distribution and full salinity and DOM fluorescence ranges of the central Arctic Ocean data set published in Stedmon et al. (2021).

1 Tg yr^{-1} when accounting for the lower DSOW volume flux of 2 Sv used (Benner et al. 2005). Comparing our export estimate to the annual discharge of carbon from the six major Arctic rivers (the Lena, Yenisei, Ob, Yukon, Mackenzie, and Kolyma Rivers), which jointly supply 19.9 Tg carbon to the central Arctic Ocean (Stedmon et al. 2011) puts the estimated export in context. Our observations suggest that 9.9% of the riverine material persists to be sequestered into the deep ocean with DSOW.

Our analysis rests on the assumption that the DOM signal is unmodified during transport from source to overflow. Given extensive sea-ice cover and that the majority of DOM is present in halocline waters below the surface mixed layer, there is low exposure to irradiance and photochemical degradation of DOM fluorescence is expected to be minimal (Amon et al. 2003). Microbial processing of organic matter (autochthonous production) would result in a weak net increase in fluorescence. Along with the entrainment of sea-ice and glacial meltwaters, this likely contributes to some of the spread in the data, while not influencing the overarching trend with salinity.

A high-resolution eddy-rich model of the Arctic and Atlantic corroborates the observational evidence for biogeochemical connectivity between Siberian river runoff and the deep waters of the Labrador Sea (Fig. 4). Passive tracers released in the near-surface layer at Siberian rivers tag the buoyant river runoff in the model. The pathway identified from the observed DOM-S relationship is clearly replicated in the model (Fig. 4), where the tracer is concentrated in the upper 200 m during its transit across the central Arctic Ocean and along East Greenland. Albeit greatly diluted, the tracer is also present at this depth range west of Greenland along the West Greenland Current and Labrador Current (Fig. 4a). The model further shows elevated tracer concentrations at depth south of the Greenland-Scotland Ridge (Fig. 4b). Here, the tracer spreads cyclonically along the western boundary following the North Atlantic Deep Water pathway. The tracer does not spread below 1000 m north of the ridge, implying entrainment into the deeper layers occurs at Denmark Strait.

Pathways and fate of Arctic freshwater and organic carbon

It is known that riverine freshwater and organic carbon from Siberian rivers are transported across the central Arctic Ocean with the Transpolar Drift and exported via Fram Strait as Polar Surface Water (Granskog et al. 2012; Stedmon et al. 2021; Gamrani et al. 2023). The same DOM signal was traced further downstream in Northeast Greenland fjords (Stedmon et al. 2015), and recently stable water isotope ratios of deuterium and oxygen confirmed Lena River water on the Northeast Greenland Shelf (Willcox et al. 2023). The further

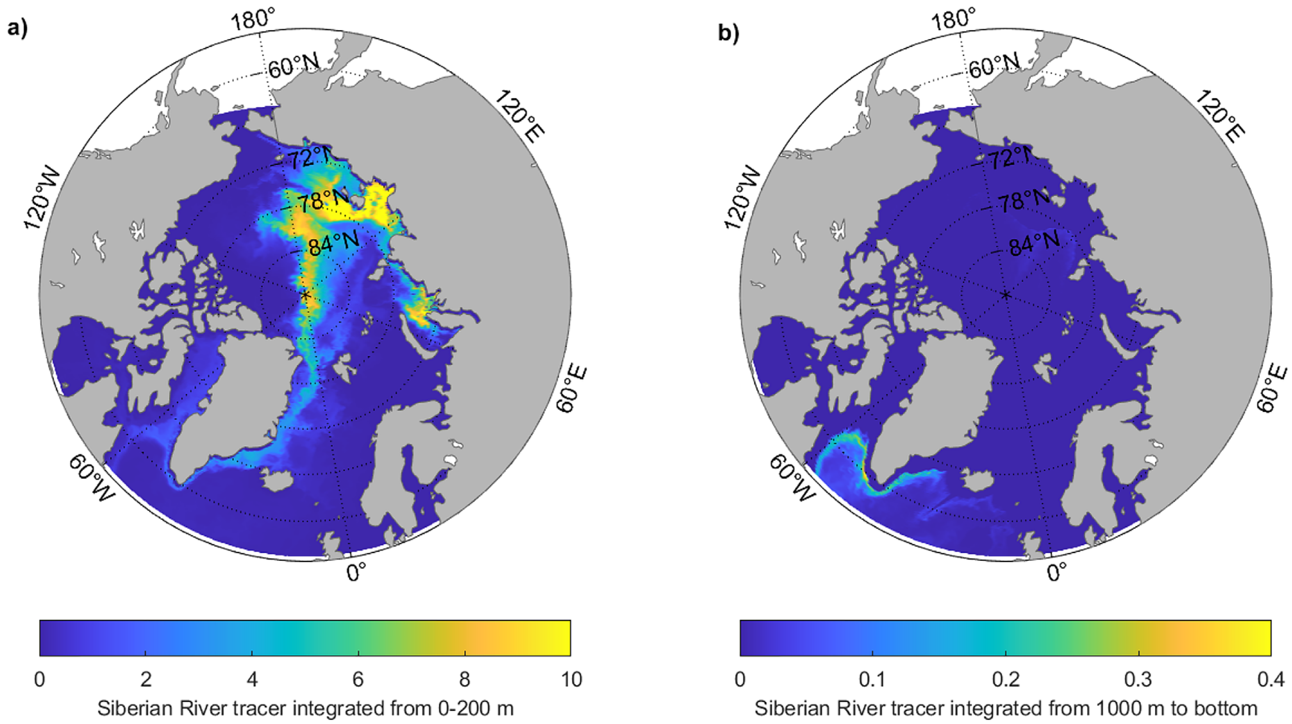

Fig. 4. Siberian river tracer concentration from the high-resolution ANHA12 ECP024 model. Panel (**a**) shows the tracer integrated over the 0–200 m depth range and panel (**b**) from 1000 m to the bottom for output on September 22, 2004. Note that choosing a different date or depth range does not change the results qualitatively. See animated fields of the tracer concentration here https://doi.org/10.7939/r3-59t1-ff14.

pathway toward the Denmark Strait is unclear. There are limited observations available to aid in the interpretation of how these relatively light waters are incorporated into the waters that constitute DSOW. However, based on results from the passive tracer, we surmise that this process occurs at Denmark Strait, given the absence of tracer below 1000 m in the Nordic Seas (Fig. 4b). In this view, the East Greenland Current is responsible for transporting DOM-rich fresh Arctic outflow to Denmark Strait. Because water parcels seaward of the East Greenland shelf break are more susceptible to advection into the interior Nordic Seas basins, we suggest that the majority of the southward transport occurs over the Northeast Greenland Shelf, where the flow is more coherent toward the Denmark Strait (Foukal et al. 2020).

This notion is consistent with the current understanding of DSOW source waters originating partially from the Greenland Sea and fed toward the Denmark Strait with the North Icelandic Jet and partially from the dense component of the East Greenland Current and separated East Greenland Current (Våge et al. 2011; Huang et al. 2020). The DSOW does not undergo significant modification from Southeast Greenland to the abyssal layer in the Labrador Sea (Yashayaev and Dickson 2008). Thus, whilst the Siberian Shelf water contribution is small—it makes up just ~1% of DSOW—it is trackable at depth in the Labrador Sea more than 6000 km from its source.

Our study reinforces previous findings on the connectivity between Arctic rivers and DSOW, based on lignin content in deep water samples from the Denmark Strait and Irminger Sea (Benner et al. 2005). Notably, we have advanced this understanding by demonstrating that the connectivity is quantifiable from in situ DOM fluorescence. Our source identification indicates that freshwater in DSOW is of riverine origin as opposed to sea-ice or precipitation. In addition, these findings offer promising prospects for monitoring the export of freshwater, oxygen, and organic carbon in the lower limb of the AMOC. The approach is suitable for autonomous observation platforms, including moorings, gliders, and floats, and holds the potential for elucidating freshwater dispersion across the Arctic and subarctic, thereby contributing to the broader discussion on freshwater impacts on the AMOC.

Data availability statement

Hydrographic data are available from data.dtu.dk with the identifier 10.11583/DTU.24991326. The model code based on the NEMO model is available at https://www.nemo-ocean.eu/. Details on the ANHA configuration are available at https://canadian-nemo-ocean-modelling-forum-commuity-of-practice.readthedocs.io/en/latest/Institutions/UofA/Configurations/ANHA12/index.html.

References

Amon, R. M. W., and R. Benner. 2003. Combined neutral sugars as indicators of the diagenetic state of dissolved organic matter in the Arctic Ocean. Deep-Sea Res. I: Oceanogr. Res. Pap. **50**: 151–169. doi:10.1016/S0967-0637(02)00130-9

Amon, R. M. W., G. Budéus, and B. Meon. 2003. Dissolved organic carbon distribution and origin in the Nordic seas: Exchanges with the Arctic Oean and the North Atlantic. J. Geophys. Res.: Oceans **108**: 3221. doi:10.1029/2002jc001594

Anderson, L. G., and R. M. W. Amon. 2015. DOM in the Arctic Ocean, p. 609–633. *In* D. A. Hansell and C. A. Carlson [eds.], Biogeochemistry of marine dissolved organic matter, 2nd ed. Academic Press. doi:10.1016/B978-0-12-405940-5.00014-5

Benner, R., P. Louchouarn, and R. M. W. Amon. 2005. Terrigenous dissolved organic matter in the Arctic Ocean and its transport to surface and deep waters of the North Atlantic. Glob. Biogeochem. Cycles **19**: GB2025. doi:10.1029/2004GB002398

Broecker, W. S. 1974. "NO", a conservative water-mass tracer. Earth Planet. Sci. Lett. **23**: 100–107. doi:10.1016/0012-821X(74)90036-3

Buckley, M. W., and J. Marshall. 2016. Observations, inferences, and mechanisms of the Atlantic Meridional Overturning Circulation: A review. Reviews of geophysics **54**: 5–63. doi:10.1002/2015RG000493

Catalá, T. S., and others. 2015. Turnover time of fluorescent dissolved organic matter in the dark global ocean. Nat. Commun. **6**: 5986. doi:10.1038/ncomms6986

Dickson, R. R., and J. Brown. 1994. The production of North Atlantic Deep Water: Sources, rates, and pathways. J. Geophys. Res.: Oceans **99**: 12319–12341. doi:10.1029/94jc00530

Edmonds, H. N., Z. Q. Zhou, G. M. Raisbeck, F. Yiou, L. Kilius, and J. M. Edmond. 2001. Distribution and behavior of anthropogenic ^{129}I in water masses ventilating the North Atlantic Ocean. J. Geophys. Res.: Oceans **106**: 6881–6894. doi:10.1029/1999jc000282

Fichefet, T., and M. A. M. Maqueda. 1997. Sensitivity of a global sea ice model to the treatment of ice thermodynamics and dynamics. J. Geophys. Res.: Oceans **102**: 12609–12646. doi:10.1029/97JC00480

Foukal, N. P., R. Gelderloos, and R. S. Pickart. 2020. A continuous pathway for fresh water along the East Greenland shelf. Sci. Adv. **6**: eabc4254. doi:10.1126/SCIADV.ABC4254

Gamrani, M., J. Eert, W. J. Williams, and C. Guéguen. 2023. A river of terrestrial dissolved organic matter in the upper waters of the central Arctic Ocean. Deep-Sea Res. I: Oceanogr. Res. Pap. **196**: 104016. doi:10.1016/j.dsr.2023.104016

Gonçalves-Araujo, R., C. A. Stedmon, B. Heim, I. Dubinenkov, A. Kraberg, D. Moiseev, and A. Bracher. 2015. From fresh to marine waters: Characterization and fate of dissolved organic matter in the Lena River Delta region, Siberia. Front. Mar. Sci. **2**: 00108. doi:10.3389/fmars.2015.00108

Granskog, M. A., C. A. Stedmon, P. A. Dodd, R. M. W. Amon, A. K. Pavlov, L. De Steur, and E. Hansen. 2012. Characteristics of colored dissolved organic matter (CDOM) in the Arctic outflow in the Fram Strait: Assessing the changes and fate of terrigenous CDOM in the Arctic Ocean. J. Geophys. Res.: Oceans **117**: C12021. doi:10.1029/2012JC008075

Hu, X., P. G. Myers, and Y. Lu. 2019. Pacific water pathway in the Arctic Ocean and Beaufort Gyre in two simulations with different horizontal resolutions. J. Geophys. Res.: Oceans **124**: 6414–6432. doi:10.1029/2019JC015111

Huang, J., R. S. Pickart, R. X. Huang, P. Lin, A. Brakstad, and F. Xu. 2020. Sources and upstream pathways of the densest overflow water in the Nordic Seas. Nat. Commun. **11**: 5389. doi:10.1038/s41467-020-19050-y

Jørgensen, L., C. A. Stedmon, T. Kragh, S. Markager, M. Middelboe, and M. Søndergaard. 2011. Global trends in the fluorescence characteristics and distribution of marine dissolved organic matter. Mar. Chem. **126**: 139–148. doi:10.1016/j.marchem.2011.05.002

Jørgensen, L., C. A. Stedmon, M. A. Granskog, and M. Middelboe. 2014. Tracing the long-term microbial production of recalcitrant fluorescent dissolved organic matter in seawater. Geophys. Res. Lett. **41**: 2481–2488. doi:10.1002/2014GL059428

Lawaetz, A. J., and C. A. Stedmon. 2009. Fluorescence intensity calibration using the Raman scatter peak of water. Appl. Spectrosc. **63**: 936–940. doi:10.1366/000370209788964548

Le Bras, I., F. Straneo, M. Muilwijk, L. H. Smedsrud, F. Li, M. Susan Lozier, and N. Penny Holliday. 2021. How much Arctic fresh water participates in the subpolar overturning circulation? J. Phys. Oceanogr. **51**: 955–973. doi:10.1175/JPO-D-20-0240.1

Madec, G. 2008. NEMO ocean engine. *In* Note du Pole de modelisation. Institut Pierre-Simon Laplace (IPSL).

Opher, J. G., J. A. Brearley, S. R. Dye, R. S. Pickart, I. A. Renfrew, B. E. Harden, and M. P. Meredith. 2022. The annual salinity cycle of the Denmark Strait overflow. J. Geophys. Res.: Oceans **127**: e2021JC018139. doi:10.1029/2021JC018139

Stedmon, C. A., and N. B. Nelson. 2015. The optical properties of DOM in the ocean, p. 481–508. *In* Biogeochemistry of marine dissolved organic matter, 2nd ed. Academic Press. doi:10.1016/B978-0-12-405940-5.00010-8

Stedmon, C. A., R. M. W. Amon, A. J. Rinehart, and S. A. Walker. 2011. The supply and characteristics of colored dissolved organic matter (CDOM) in the Arctic Ocean: Pan Arctic trends and differences. Mar. Chem. **124**: 108–118. doi:10.1016/j.marchem.2010.12.007

Stedmon, C. A., M. A. Granskog, and P. A. Dodd. 2015. An approach to estimate the freshwater contribution from glacial melt and precipitation in East Greenland shelf waters

using colored dissolved organic matter (CDOM). J. Geophys. Res.: Oceans **120**: 1107–1117. doi:10.1002/2014JC010501
Stedmon, C. A., and others. 2021. Insights into water mass origins in the Central Arctic Ocean from in-situ dissolved organic matter fluorescence. J. Geophys. Res.: Oceans **126**: e2021JC017407. doi:10.1029/2021JC017407
Tanhua, T., K. A. Olsson, and E. Jeansson. 2005. Formation of Denmark Strait Overflow Water and its hydro-chemical composition. J. Mar. Syst. **57**: 264–288. doi:10.1016/j.jmarsys.2005.05.003
Våge, K., R. S. Pickart, M. A. Spall, H. Valdimarsson, S. Jónsson, D. J. Torres, S. Østerhus, and T. Eldevik. 2011. Significant role of the North Icelandic jet in the formation of Denmark Strait overflow water. Nat. Geosci. **4**: 723–727. doi:10.1038/ngeo1234
Walker, S. A., R. M. W. Amon, and C. A. Stedmon. 2013. Variations in high-latitude riverine fluorescent dissolved organic matter: A comparison of large Arctic rivers. J. Geophys. Res. Biogeosci. **118**: 1689–1702. doi:10.1002/2013JG002320
Willcox, E. W., and others. 2023. An updated view of the water masses on the Northeast Greenland shelf and their link to the Laptev Sea and Lena River. J. Geophys. Res.: Oceans **128**: e2022JC019052. doi:10.1029/2022JC019052
Yamashita, Y., and E. Tanoue. 2008. Production of bio-refractory fluorescent dissolved organic matter in the ocean interior. Nat. Geosci. **1**: 579–582. doi:10.1038/ngeo279
Yashayaev, I., and B. Dickson. 2008. Transformation and fate of overflows in the northern North Atlantic, p. 505–526. *In* R. R. Dickson, J. Meincke, and P. Rhines [eds.], Arctic-Subarctic Ocean fluxes: Defining the role of the northern seas in climate. Springer. doi:10.1007/978-1-4020-6774-7_22

Acknowledgments

This study was funded by Independent Research Fund Denmark Grant No. 9040-00266B (CAS), Carlsberg Foundation Grant No. CF22-0142 (CAS), Nordic Council of Ministers AG-Fisk Grant No. (209)-2020-LEGCO (CAS), Natural Sciences and Engineering Research Council (NSERC) of Canada Discovery Grant (rgpin 227438-09) (PGM), and U.S. National Science Foundation Grant OPP-1902595 (CML, KAS).

Conflict of Interest

None declared.

Submitted 27 May 2024
Revised 22 July 2024
Accepted 08 September 2024

Associate editor: James J. Leichter